An IR Matrix Isolation and DFT Theoretical Study of the First Steps of the Ti(0) Ethylene Reaction: Vinyl Titanium Hydride and Titanacyclopropene

Yu Kang Lee and Laurent Manceron*

Laboratoire de Spectrochimie Moléculaire, CNRS URA 508, Université Pierre et Marie Curie, case courrier 49, 4 place Jussieu, 75252 Paris Cedex 05, France

Imre Pápai

Institute of Isotopes of the Hungarian Academy of Sciences, Spectroscopy Department, H-1525 Budapest, P.O.B. 77, Hungary

Received: June 9, 1997; In Final Form: September 22, 1997[⊗]

Two new species have been formed by codeposition of ground-state Ti atoms and ethylene molecules in excess argon at low temperature, followed by selective electronic excitation of the Ti atoms. The two products are identified as $H_2Ti(C_2H_2)$ (titanacyclopropene) and $HTi(C_2H_3)$ (vinyltitanium monohydride) based on IR spectroscopy with various isotopic precursors ($^{12}C_2H_4$, $^{13}C_2H_4$, C_2D_4, CH_2CD_2, and the natural Ti isotopes), vibrational analysis, and density functional theory (DFT) calculations. Theoretical results are also presented for a $Ti(C_2H_4)$ π-complex structure, not observed in this study. Although DFT predicts a strongly bound $Ti(C_2H_4)$ system having a stability similar to $H_2Ti(C_2H_2)$ and $HTi(C_2H_3)$, this molecule is not observed in our experiments. It is found that Ti atoms react with ethylene when in the first excited states (^{3}F, ^{3}D, or ^{3}G) to form first an insertion product and next, after a 1,2-hydrogen shift, the dihydrotitanacyclopropene.

I. Introduction

The interest shown in organometallic derivatives of low-valent titanium (with formal oxidation states less than IV) is due to the activity of organotitanium species of this type in Ziegler−Natta alkene polymerization reactions.[1] The presently admitted conception that olefin polymerization is initiated at a titanium−carbon bond increases the importance of well-defined, low-valent organotitanium molecules, and these offer models of the structures and properties of larger compounds important for hydrogenation or organometallic syntheses.[2] Some important advances have been made in the characterization of low-valent Ti compounds following the first syntheses of arene complexes using "direct" metal vapor synthesis,[3] paving the way for conventional preparative methods involving reduction of the metal chloride in solutions.[4] Later, several workers using matrix isolation continued on the same idea[5] and prepared other reactive or undercoordinated hydride[6,7] or carbonyl species.[8,9] However, to our knowledge, no study has yet been devoted to reaction products of simple alkene molecules with Ti(0) and the synthesis of elementary compounds containing titanium−carbon bonds.

We present here an IR spectroscopic study of the reaction products of Ti atoms with the simplest alkene, ethylene, isolated in rare gas. Results obtained from density functional theory (DFT) calculations on possible reaction products are also reported in this paper to confirm the identification of the observed species, to determine their equilibrium structures, and finally to understand the bonding mechanisms in these new molecules.

II. Experimental and Computational Details

The experiments were performed using a high-vacuum stainless steel cryostatic vessel and a titanium evaporation device fitted directly in a 150 mm diameter vacuum chamber evacuated by a Leybold 1000 L/s diffusion pump equipped with a large capacity liquid nitrogen trap. The base pressure before starting an experiment, after outgassing but with the titanium filament hot, was always less than 5×10^{-7} mbar.

About 5.5 mmol of a mixture of ethylene and argon (1/100 to 1/4000 molar ratios) were deposited in 2 h onto one of the four sides of a flat, highly polished, chromium-plated copper mirror cube maintained around 10 K by an APD displex system. The samples were probed in the transmission-reflection mode by the infrared beam of a Bruker 120 FTIR spectrometer with a resolution varied between 0.5 and 0.1 cm^{-1} using a HgCdTe detector and a KBr/Ge beam splitter in the 4500−500 cm^{-1} range, and with 0.5 cm^{-1} resolution in the 500−150 cm^{-1} region using a silicon bolometer and a Mylar beam splitter. Each sample spectrum was processed against a bare mirror background recorded at 10 K just before sample deposition and was baseline-corrected to compensate for infrared light scattering.

Broad and narrow band excitations were achieved using a 200 W high-pressure mercury−xenon arc lamp and either cutoff colored glass filters or narrow band (10 nm fwhm) interference filters were used for selective excitations.

Titanium was vaporized from a piece of 1.0 mm diameter Ti−Mo 85/15 alloy wire (Goodfellow) in the 1500−1700 °C range. The metal effusion rate was continuously monitored using a quartz microbalance and varied between 9 and 120 $\times$ 10^{-8} g/min.

High-purity argon (Prodair, 99.995%), C_2H_4 (Air Liquide, 99.50%), C_2D_4 (MSD, 99.20% D), and $^{13}C_2H_4$ (MSD > 90.0%) were used without further purification but after several freeze−pump−thaw cycles to minimize possible atmospheric contamination. Another isotopic species of ethylene (1,1-D_2) was prepared by the Wittig reaction of deuterated formaldehyde with triphenylmethylphosphonium according to the procedure described by Atkinson et *al.*[10] The purity of this product was checked using IR spectroscopy. Its main impurities ($CHD{=}CD_2$ and $CH_2{=}CHD$) were in quantities weak enough (about 1.7% and 2%, respectively) to be neglected.

All calculated properties of the investigated systems were

[⊗] Abstract published in *Advance ACS Abstracts,* November 15, 1997.

S1089-5639(97)01870-7 CCC: $14.00

obtained at the gradient-corrected level of DFT. The calculations were carried out using the BP86 functional[11,12] and the (63321/5211/41), (5211/411/1), and (41/1) Gaussian orbital basis sets (for Ti,[13] C,[14] and H,[14] respectively) as implemented in the deMon code.[15−17] For some of the molecules—in cases where we suspected an unusual sensitivity of the calculated properties with respect to the applied exchange−correlation functional and the basis set—we repeated the calculations with the B3LYP functional[18,19] using the above basis sets, and/or the 6-311G** bases (i.e., the standard 6-311G** basis sets for C and H, and the Wachters−Hay all-electron basis sets for Ti).[20] These calculations were carried out with the Gaussian 94 package.[20] Although there are some indications from recent studies[21−23] that the B3LYP functional gives more accurate predictions for binding energies of transition metal−ligand systems than the standard gradient-corrected functionals, there is still no clear evidence that it provides the highest quality results for vibrational data. Since the BP86 functional proved to give reasonably accurate frequencies for transition metal−monoligand molecules,[24] we decided to use this level of theory in the present study as well. Therefore, except where stated otherwise in the text, all results reported here will refer to BP86 (deMon) calculations.

The technical details (the numerical quadrature grid, the algorithms applied in the geometry optimization, and the vibrational analysis) of the deMon calculations were given in ref 25. In Gaussian 94 calculations, the default integration grid (including about 7000 points per atom) was used, the geometries were optimized with the Berny algorythm, and the harmonic frequencies were obtained from the analytical second derivatives.

III. Results

A. Experimental Results. When comparing the IR spectrum of ethylene-containing matrix samples prepared with and without Ti atoms, some new bands, characteristic of reaction products, can be found directly after reagent deposition, which are supposedly in their ground states. However, although the experimental conditions such as the Ti or C_2H_4 concentrations and the deposition time and temperature were kept the same in some of our experiments, the observed intensities were not always reproducible when changing the shape or length of the metal-emitting filament source. It is thus supposed that, in addition to the titanium and ethylene concentrations, other parameters exist that could not be directly controlled and visualized easily such as the temperature and form of the metal source. These parameters have probably influenced the product yield because of variable light intensities emitted by the hot filament source. Therefore, experiments were run in order to check the possibility of photochemically induced reactions. According to the experimental data of Gruen and co-workers,[26] the first electronic states of Ti atom could be reached via optical excitation at about 510 and 490 nm ($z^3F_2^0$, $z^3F_3^0$, $z^3D_1^0$, $z^3D_2^0$) for one group, and for the second group, at about 460 nm ($z^3G_3^0$, $z^1F_3^0$). One set of new absorptions (species A) can be detected directly upon deposition (see trace b in Figure 1, the most intense absorption at 1585.4 cm^{-1}), but grows strongly after specific irradiation at wavelengths above 400 nm (Figure 1, trace c). A second group appears after irradiation only and is labeled B. The most intense absorption of B (at 1500.0 cm^{-1}) is, after deposition, hardly detectable within the noise level (see Figure 1).

The irradiation in the wavelength range above 700 nm caused but a minute growth of species A, more marked above 600 nm. A further expansion of the wavelength ranges to 500 and 400 nm caused a marked growth of both species, but with different

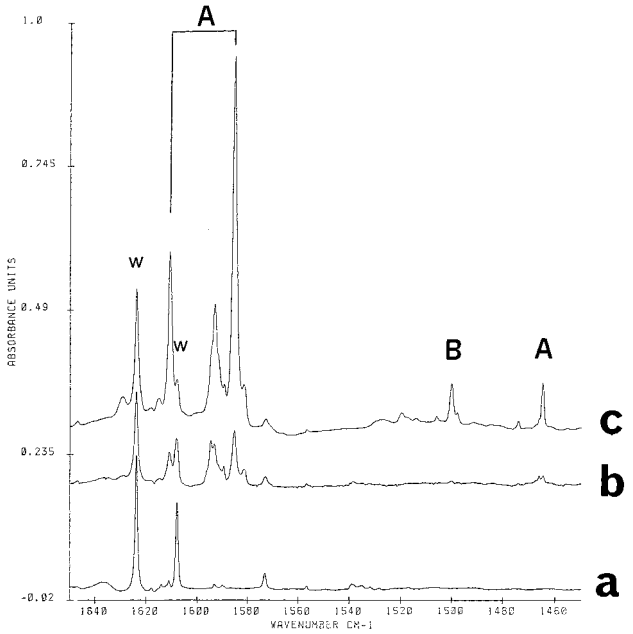

Figure 1. IR spectra of the region 1650−1450 cm^{-1} showing the preliminary formation of the Ti + C_2H_4 reaction products. (a) Sample deposited without ethylene, 1/3000 Ti/Ar. (b) Sample with C_2H_4 after deposition, 1/5/1000 Ti/C_2H_4/Ar. (c) After irradiation using broad band irradiation with wavelength >400 nm. W indicates water impurity absorptions, A and B labels refer to $H_2TiC_2H_2$ and $HTiC_2H_3$, respectively, as explained in the text.

rates. We observed about a 4-fold intensity increase for A species bands and 22-fold increase for B when we compared the bands intensities after 10 min irradiation in the range above 400 nm to those just after deposition. Species B is unaffected by irradiation in the wavelength range above 600 nm and appeared only after excitation in the wavelength range up to 500 or 400 nm. Nevertheless, a continuous irradiation in the range above 400 nm caused at first the growth of A and B species bands and then destructed them gradually, indicating competing formation, conversion, and/or destruction processes.

In order to study in more detail the formation channels, more specific monochromatic excitations had to be performed. Irradiating first at 546 or 522 nm could develop species B without forming species A. However, 514 or 480 nm light build up these two species simultaneously but with an increasing yield (Figure 2). Once both A and B species have been formed, 466 nm irradiation could convert species B into species A. On the other hand, 546 nm light fostered species B, at the expense of species A, that is, it operates the back-conversion.

Once the optimum conditions have been found to characterize A and B species, identical experiments were repeated, varying *only* the titanium or ethylene molar ratios (from 1/100 to 1/4000 for ethylene, from 1/250 to 1/3000 for titanium). No difference appeared in the titanium or ethylene dependences of the A or B species relative intensities. Moreover, both species could still be observed, even in the sample grown with the lowest reactant concentrations. On these grounds, it can be established that species A and B are two isomeric forms of the 1/1 Ti/C_2H_4 reaction product. Likewise, comparable experiments were run using C_2D_4, $^{13}C_2H_4$, and CH_2CD_2 as isotopic precursors (Figures 3−5). The frequencies and relative intensities for all isotopic species of A and B are reported in Table 1.

For most vibrations, the isotopic shifts are straightforward to follow, but some observations are complicated by overlapping or site effects and therefore deserve special comments.

For Species A. The assignment of the 328 cm^{-1} band is ambiguous because of overlapping with some B species signals

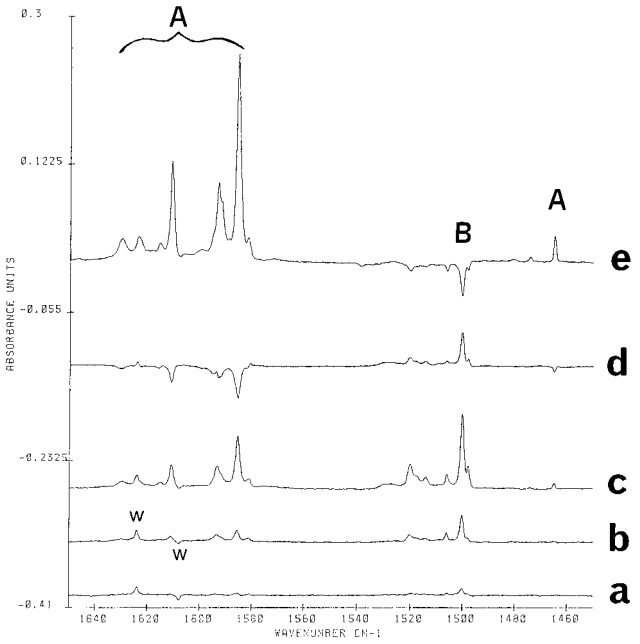

Figure 2. Infrared difference spectra of the 1650−1450 cm^{-1} region displaying the formation and photochemical behaviors of the two species $H_2TiC_2H_2$ (A) and $HTiC_2H_3$ (B) using selective monochromatic excitation. (a) After 522 nm excitation, minus after deposition. (b) After minus before 514 nm light excitation. (c) After minus before 480 nm light excitation. (d) After minus before 546 nm light excitation. (e) After minus before 466 nm light excitation W designates difference bands due to spin conversion of H_2O traces.

and also because of the absence of clearly correlated absorption when using $^{13}C_2H_4$. Nevertheless, a TiC_2D_4 counterpart appears at 292 cm^{-1}.

We also observed some relatively smaller peaks appearing on the side of several bands beside the most intense absorption peaks. These sidebands did not always have exactly the same irradiation behavior as the main absorptions bands (Figure 2) and were very sensitive to warmup effects, even with relatively mild annealing between 15 and 20 K, but all had an identical behavior upon isotopic substitution and are therefore attributed to various unstable trapping sites. Multiplets arising from such multiple trapping sites of the same bands have been indicated in brackets in Table 1, as they could be evidenced from temperature effects. Notably, the magnitude of the site splittings vary from one fundamental to the other. The effect of a slight annealing on the multiple trapping sites of species A is particularly dramatic on some fundamentals. Figure 4 shows the effect of a 15 K temperature increase on the high-frequency motions of A with C_2D_4 precursor. The bands shift a few wavenumbers and are drastically narrowed in a better crystallized environment. A characteristic quintet pattern thus emerges exhibiting about 0.8 cm^{-1} splittings (0.5 cm^{-1} with C_2H_4). The relative intensities on these multiplets follow well that of the abundancies of the naturally occurring isotopes of titanium (see Figure 4, trace c).

Most of the absorptions of species A were weaker with the CH_2CD_2 isotopic precursor. Below the peak at 1154.3 cm^{-1}, we observed 7 bands. The assignment of the 831.5 cm^{-1} band is uncertain because it presents inconsistent relative intensities, although it qualitatively has the same behavior as species A throughout the interconversion process.

For Species B. The strongest absorption of this species is measured at 1500 cm^{-1} with no measurable $^{12}C/^{13}C$ shift. A small absorption appears at 1568.7 cm^{-1} for the ^{13}C labeled isotopic species. Observation of a corresponding signal with C_2H_4, higher in the region around 1600 cm^{-1} would anyhow

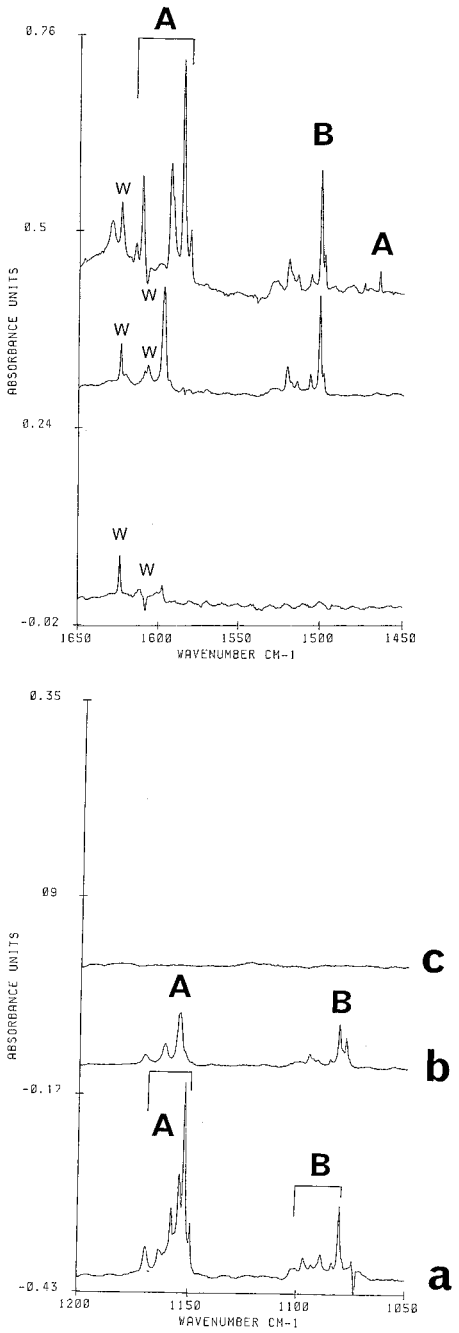

Figure 3. IR spectra of the 1650−1450 cm^{-1} and 1200−1050 cm^{-1} region for different isotopic species after irradiation with monochromatic 480 nm light. (a) 1/5/1000 $Ti/C_2D_4/Ar$. (b) 1/5/1000 $Ti/CH_2CD_2/Ar$. (c) 1/5/1000 $Ti/C_2H_4/Ar$.

be difficult due to the presence of water impurity peaks. Likewise, we did not find with the protonated precursors any obvious counterpart to the 981.4 cm^{-1} band observed with the C_2D_4 precursor. Similarly, two bands are observed at 665.3 and 632.9 cm^{-1} with Ti/C_2D_4 but only one absorption was observed for the protonated species in the corresponding region (867.7 cm^{-1} for ^{12}C and 866.9 cm^{-1} for ^{13}C). On the other hand, we found only three Ti/C_2D_4 species bands in the far-IR region corresponding to four bands with either $Ti/^{12}C_2H_4$ or $Ti/^{13}C_2H_4$, but the 190 cm^{-1} cutoff of the CsI window used in our experiments prevented observations below that frequency.

B. Theoretical Results. Three Ti/C_2H_4 reaction products have been investigated theoretically in our study, namely, the $Ti(C_2H_4)$, $HTi(C_2H_3)$, and $H_2Ti(C_2H_2)$ molecules. Our results obtained from DFT calculations for these systems are presented in the following subsections.

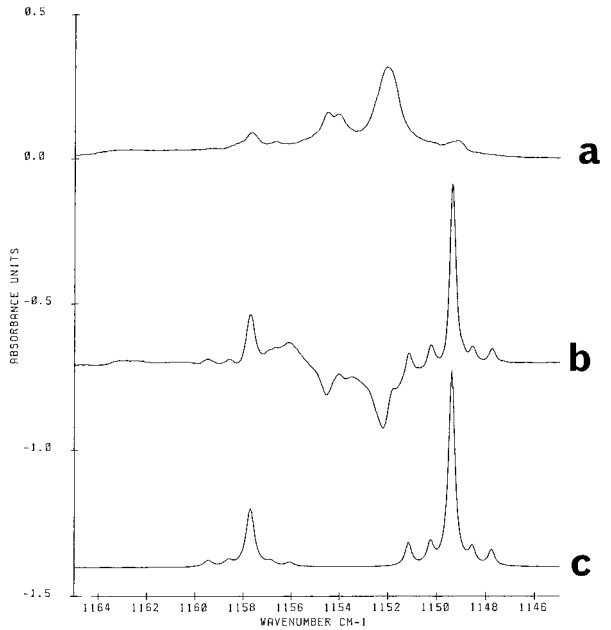

Figure 4. Infrared spectra for the Ti−D stretching region of the D_2-TiC_2D_2 species. (a) After deposition and 480 nm excitation. (b) Difference spectrum, after minus before annealing the sample at 25 K. (c) Synthetic spectrum using 0.28 cm^{-1} Lorentzian band shapes, relative intensities following the titanium natural isotopic abundances, and the isotopic shifts calculated using the semiempirical force field (see text).

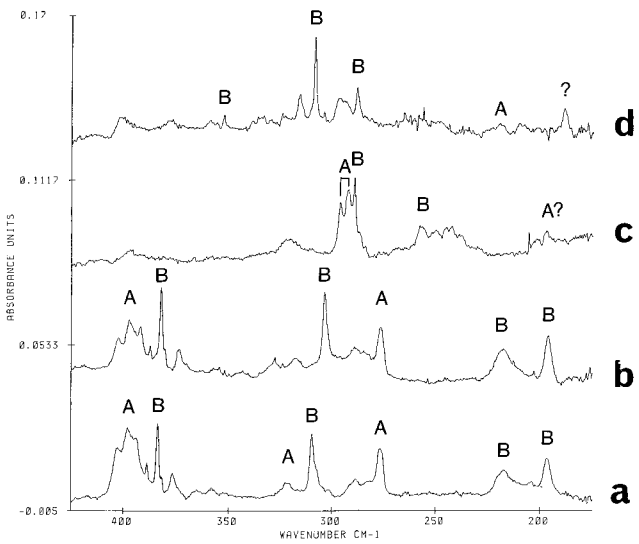

Figure 5. Far-infrared spectra for various isotopic species of $H_2TiC_2H_2$ (A) and $HTiC_2H_3$ (B). All spectra are taken after 480 nm light excitation. (a) 1/5/1000 $Ti/C_2H_4/Ar$. (b) 1/5/1000 $Ti/^{13}C_2H_4/Ar$. (c) 1/5/1000 $Ti/C_2D_4/Ar$. (D) 1/5/1000 $Ti/CH_2CD_2/Ar$.

1. The Ti(C_2H_4) Molecule. We have carried out geometry optimization and vibrational analysis for singlet, triplet, and quintet spin states of $Ti(C_2H_4)$, all having C_{2v} symmetry. The predicted properties for the lowest states are collected in Table 2.

The ground state of $Ti(C_2H_4)$ is $^3B_1$, followed by the $^1A_1$ and $^5A_1$ states, which lie 4 and 8 kcal/mol above the ground state, respectively. All these states appear to be quite strongly bound relative to the ground-state Ti atom (s^2d^2 (^3F)) + C_2H_4, since the Ti−C_2H_4 binding energy calculated with respect to ground-state reagents is 45 kcal/mol, which might be, however, an overestimated value.[27]

Table 2 also reveals that the equilibrium geometries obtained for the $^1A_1$ and $^3B_1$ states on one hand, and for the $^5A_1$ state on the other, are rather different. The Ti−C bond in $^5B_1$ is about 0.3 Å longer than those in the $^1A_1$ and $^3B_1$ states, and the distortion of the C_2H_4 unit (with respect to free C_2H_4) is far more significant in the latter two states. This is in line with the results of the MCPF (modified coupled pair functional study) on the second-row transition metal $M(C_2H_4)$ molecules,[28] where the difference between the equilibrium properties of the low- and high-spin states of $M(C_2H_4)$ molecules calculated for the metal atoms to the left-hand side of the periodic table was attributed to a difference in the binding mechanisms. The binding in the $^1A_1$ and $^3B_1$ states of $Ti(C_2H_4)$ has a covalent character (the calculated Ti−C bond orders are about 1.0) and the C−C π-bond is essentially broken (C−C bond order of about 1.0), whereas the $^5A_1$ state can rather be described as a Ti-ethylene π-complex (the Ti−C and C−C bond orders are about 0.5 and 1.5, respectively).

The difference between the two types of $Ti(C_2H_4)$ molecules is apparent from the predicted IR spectra as well, since (1) the CC stretching frequencies for the $^1A_1$ and $^3B_1$ states are around 1000 cm^{-1}, while it is at 1230 cm^{-1} for $^5A_1$; and (2) both the symmetric and asymmetric TiC stretching frequencies are much higher in the "low-spin" states. The calculated IR spectrum of the ground-state molecule is characterized by two medium intense absorptions in the CH stretching region and bands around 970 cm^{-1} (CC stretching), 510 cm^{-1} (symmetric TiC stretching), and 450 cm^{-1} (CH_2 tilt) with similar intensities. All the remaining bands are rather weak.

2. The HTi(C_2H_3) Molecule. We have considered all three spin states ($2S + 1 = 1$, 3, and 5) for the $HTi(C_2H_3)$ molecule and found the triplet state to be the most stable, lying 8 kcal/mol above the ground state of $Ti(C_2H_4)$. The lowest singlet state of $HTi(C_2H_3)$ is only 8 kcal/mol less stable than the ground state, but the quintet state is separated by at least 65 kcal/mol from the triplet state. Because of its thermodynamical instability, the formation of the quintet state of the $HTi(C_2H_3)$ molecule in the experiments is very unlikely, and for this reason we present results only for the singlet and triplet states. The optimized geometries and the predicted IR spectra for these two states are given in Table 3, while the corresponding equilibrium structures and the calculated bond orders are depicted in Figure 6.

Despite comparable stabilities, the equilibrium structures of the singlet and triplet states of $HTi(C_2H_3)$ are entirely different. The optimized bond lengths and the related bond orders suggest that the singlet molecule is in fact a cyclopropene derivative, where one of the sp^2 carbon atoms is substituted by Ti, whereas the triplet state is a vinyl hydride, in which the Ti atom weakly interacts with the carbon and one of the hydrogen atoms of the CH_2 group. None of the two structures have symmetry elements, because the TiH bonds are out of the TiCC plane. However, the triplet state has a nearly planar geometry with an $HTiC_1C_2$ dihedral angle of 168° and for the sake of simplicity its normal modes will be classified as in-plane and out-of-plane vibrations.

Since the predicted IR spectra for both states will be compared to the experimental data in the next section, it is worthwhile to point out the main differences between them. First the TiH stretching bands are the most intense bands for both states, all the other modes having significantly lower IR intensities. As a result of the Ti···H interaction, one of the CH bands of the triplet $HTi(C_2H_3)$ is clearly separated from the other two, its frequency shifting down by about 300 cm^{-1}. The two spectra are rather different in the mid-infrared region. No band with considerable IR intensity is predicted for the singlet state in the 1100−1600 cm^{-1} range, but, for the triplet state, there are three medium absorptions in this region in addition to the TiH

TABLE 1: Infrared Absorptions from the Reaction of Ti Atoms with Various Ethylene Isotopic Molecules in Solid Argon[a]

Ti + C_2H_4		Ti + $^{13}C_2H_4$		Ti + C_2D_2		Ti + CH_2CD_2	
freq (cm^{-1})	relative intensity	freq (cm^{-1})	relative intensity	freq (cm^{-1})	relative intensity	freq (cm^{-1})	relative intensity
			A Species				
1629.9		1629.1				1607.5	
1623.4		1622.5				1597.3	1.00
1615.1		1614.4				1585.0	
1610.6	0.38	1610.1	0.41			1581.3	
1593.1		1592.9					
1585.4	1.00	1585.4	1.00				
1581.3		1581.3					
1474.0				1401.4			
1467.2		1422.9		1399.6		1436.4	
1464.8	0.08	1414.0	0.048	1397.4	0.035	1435.1	0.16
						1433.8	
1000.4	0.05	977.0	0.028	1169.3			
994.4		973.0		1163.5		1161.4	
990.3				1157.8	0.11	1157.9	
						1154.3	0.67
769.1		768.8		1154.3		1152.3	
765.4	0.055	765.1	0.035	1152.1	1.00	1149.5	
762.5		761.3		1149.2			
687.8	0.21	684.9	0.023	872.2	0.075	671.3	0.135
675.9		672.3		865.9		645.6	0.123
				860.9		572.7	0.026
				858.8		520.9	0.12
						494.8	0.035
667.7	0.068	663.2	0.078	613.2	0.14	219.1	0.036
598.1	0.16	585.8	0.135	606.0			
399	0.17	≈398	0.12	548.3	0.033		
328	0.016						
277	0.064	276.8	0.071	507.7	0.28		
				503.2			
				489.0	0.056		
				454.6	0.146		
				≈292	0.1		
			B Species				
		1568.7	0.023	1096.0		1520.3	
				1093.0		1514.3	
1519.7		1519.6		1088.8		1506.3	
1514.0		1514.0		1083.5		1506.3	1.00
1505.9		1505.8		1080.3	1.00	1498.2	
1500.0	1.00	1500.0	1.00				
		1497.8		981.4	0.03	1357.6	0.153
871.2				665.3	0.21	1094.9	
867.7	0.252	866.9	0.57	661.1		1091.0	
						1085.2	
582.2	0.182	568.1	0.34	632.9	0.32	1081.2	0.47
579.0						1078.2	
				531.5	0.33		
394.2		391.8		526.8		720.1	0.035
388.6		387.2					
383.6	0.231	382.1	0.142	289.4	0.26	548.8	0.30
376.7		373.5				544.8	
				256.7	0.17	539.8	
309.6	0.267	303.7	0.153	250.3			
301.6				242.6		352.2	0.03
217	0.256	217.5	0.466				
196.7	0.292	196.2	0.218			324.2	
						315.7	
						308.4	0.21
						303.9	
						288.1	0.13

[a] Relative intensities are normalized to the strongest absorption for each species.

stretching band. In turn, there are two medium intense absorptions at about 1000 cm^{-1} for the singlet state, but no band is predicted in this region for the triplet state. As another important dissimilarity, the TiC stretching band of the triplet state is at about 600 cm^{-1}, while the two TiC stretching bands of the singlet are predicted to be at about 1000 and 500 cm^{-1}.

3. The $H_2Ti(C_2H_2)$ Molecule. The singlet state is expected to be clearly the ground state for $H_2Ti(C_2H_2)$, since the four valences of Ti are saturated by forming two Ti−H and two Ti−C bonds. Indeed, we calculate the triplet state to be 31 kcal/mol above the singlet, and the lowest quintet state is about 90 kcal/mol above the ground state. It is interesting to note that the thermodynamical stability of the $H_2Ti(C_2H_2)$ molecule is essentially identical with that of ground-state $Ti(C_2H_4)$.

The calculated ground-state equilibrium structure has C_s symmetry, with a symmetry plane containing the $Ti(C_2H_2)$ unit (see Figure 7). The C_{2v} structure, in which the TiH_2 plane is perpendicular to the CC bond, turns out to be a transition state,

TABLE 2: Calculated Properties of Various Spin States of $Ti(C_2H_4)$

	singlet	triplet	quintet
R(TiC)[a]	2.028	2.026	2.320
R(CC)	1.492	1.528	1.400
R(CH)	1.110	1.114	1.106
α(HCH)	114.3	111.7	115.9
φ[b]	38.4	29.0	13.1
ΔE[c]	3.6	0.0	8.0
a_1			
ω_1 CH str	2988 (0)[d]	2943 (29)	3023 (0)
ω_2 CH_2 def	1347 (7)	1360 (0)	1487 (20)
ω_3 CC str	1045 (20)	970 (13)	1230 (42)
ω_4 CH_2 ωag	744 (3)	758 (1)	802 (2)
ω_5 TiC str	513 (10)	511 (20)	339 (1)
a_2			
ω_6 CH str	3057 (0)	2999 (0)	3092 (0)
ω_7 CH_2 rock	1121 (0)	1103 (0)	1163 (0)
ω_8 CH_2 tωist	460 (0)	428 (2)	790 (0)
b_1			
ω_9 CH str	3068 (3)	3015 (8)	3113 (1)
ω_{10} CH_2 rock	719 (0)	765 (1)	770 (2)
ω_{11} CH_2 tilt	432 (0)	446 (17)	327 (5)
b_2			
ω_{12} CH str	2983 (2)	2936 (21)	3017 (3)
ω_{13} CH_2 def	1329 (5)	1341 (3)	1383 (3)
ω_{14} CH_2 ωag	850 (4)	886 (7)	730 (3)
ω_{15} TiC str	483 (23)	453 (1)	246 (0)

[a] Bond distance (R) in angstroms, angles (α) in degrees. [b] φ is the angle between the C−C bond and the bisector of the HCH bond angle (deviation from the planar C_2H_4 structure). [c] Relative energies (in kcal/mol) relative to the triplet state. [d] Harmonic frequencies (in cm^{-1}) and IR intensities (in km/mol, in parentheses).

but with a flat TiH_2 wagging potential. In fact, the energies of the C_s and C_{2v} structures are within a few tenths of a kcal/mol. The optimized geometries and the IR spectra obtained for the two structures are given in Table 4. The results indicate that the bond lengths and most of the vibrational frequencies are not sensitive to the wagging of the TiH_2 unit. The sole vibrational mode (besides the TiH_2 wag) which has notably different frequencies in the two structures is the TiH_2 rocking mode (ω_{11}), for which the two frequencies differ by about 100 cm^{-1}. The frequency of the TiH_2 twisting mode (ω_8) does not seem to vary much when going from C_s to C_{2v}, but this is definitely not true for the corresponding IR intensities. Therefore, we do not expect the obtained harmonic frequencies and IR intensities to be accurate predictions for these low-frequency modes.

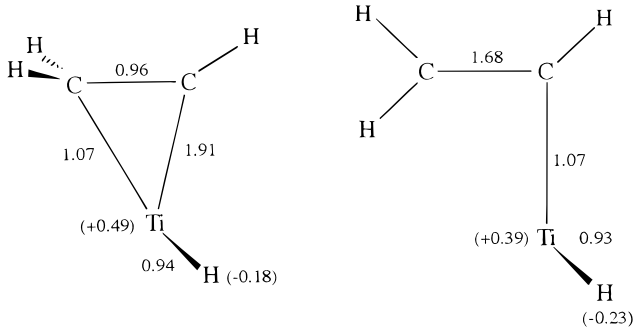

Figure 6. Calculated structures and bond orders for the singlet and triplet states of $HTiC_2H_3$ (see Table 3).

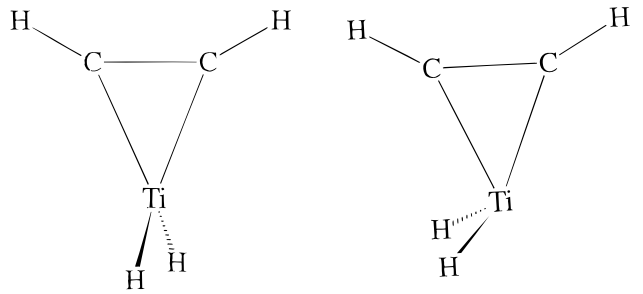

Figure 7. Calculated C_{2v} and C_s structures for $H_2TiC_2H_2$ (see Table 4 for parameters).

Table 4 also shows that the two TiH stretching bands, from which the symmetric motion (ω_2) has a slightly higher frequency, are again the most intense bands in the IR spectrum. The CH stretching bands, on the other hand, are very weak,

TABLE 3: Equilibrium Geometries and Predicted IR Spectra for Various Spin States of HTi (C_2H_3) (See Footnotes in Table 2)

	singlet	triplet
R(TiH)	1.751	1.772
R(TiC^1)[a]	1.812	2.004
R(TiC^2)[a]	1.997	2.354
R(CC)	1.525	1.357
R(CH^1)[a]	1.108	1.105
R(CH^2)[a]	1.119	1.107/1.133[b]
α(HCH)	111.8	110.2
α(CCH)	125.2	121.7
α($HTiC^1$)	102.8	129.3
α($HTiC^2$)	72.9	86.7
φ($HTiC^1C^2$)	106.7	168.3
	3056 (1) CH str	3080 (1) CH^1 str
	2931 (27) CH_2 str (asym)	3045 (7) CH^2 str
	2880 (36) CH_2 str (sym)	2763 (43) CH^2 str (Ti)
	1613 (339) TiH str	1586 (404) TiH str
	1351 (1) CH_2 bend	1560 (43) CH_2 bend + CC str
	1004 (16) TiC^1 str + CC str	1358 (47) CC str + CH_2 bend
	949 (29) CC str + TiC^1 str	1135 (25) CH & CH_2 rock (iph)
	921 (8) CH_2 rock	909 (9) CC torsion
	737 (33) CH wag	818 (30) CH & CH_2 rock (oph)
	650 (87) CH_2 wag	772 (40) CH & CH_2 wag (iph)
	511 (48) CC tilt	600 (26) TiC^1 str
	491 (98) TiC^2 str	399 (35) CC tilt
	451 (13) CH_2 twist	357 (32) HTiC bend + TiC^2 str
	395 (132) CH twist	276 (81) TiC^2 str + HTiC bend
	329 (73) HTiC bend	69 (39) HTiC bend (oop)

[a] C^1 an H^1 refer to the carbon and hydrogen atoms of the CH group, while C^2 and H^2 are those of CH_2. Bond distance (R) in angstroms, angles (α, φ) in degrees. [b] The second value refers to the H_2 atom, which weakly interacts with Ti.

TABLE 4: Equilibrium Geometries and Predicted IR Spectra for the C_s and C_{2v} Structures of the Ground State of $H_2Ti(C_2H_2)$ (See Footnotes in Table 2)

	C_s	C_{2v}
R(TiC)	1.980/1.957[a]	1.981
R(TiH)	1.747	1.755
R(CC)	1.347	1.343
R(CH)	1.108/1.107	1.107
α(HCC)	131.5/135.6	133.4
α(HTiH)	122.4	125.4
φ	128.9	180.0
a_1		
ω_1 CH str	3077 (0)	3077 (0)
ω_2 TiH str	1647 (217)	1650 (291)
ω_3 CC str + CCH def	1448 (13)	1464 (9)
ω_4 CCH def	751 (19)	747 (20)
ω_5 TiH2 def + CCH def	720 (112)	704 (96)
a_2		
ω_6 TiC str	571 (11)	574 (3)
ω_7 HCCH tors	895 (1)	882 (0)
ω_8 TiH_2 twist	285 (54)	320 (1)
b_1		
ω_9 TiH str	1639 (416)	1634 (486)
ω_{10} HCCH tilt	653 (31)	614 (55)
ω_{11} HTiH def	429 (8)	324 (1)
b_2		
ω_{12} CH str	3041 (5)	3049 (2)
ω_{13} CCH def + TiC str	1015 (74)	1017 (73)
ω_{14} TiC str + CCH def wag	620 (78)	591 (l75)
ω_{15} HTiH wag	248 (202)	*i* 171

[a] The two values refer to the "right" and "left" side of the C_2 structure (see Figure 7). Bond distance (*R*) in angstroms, angles (α) in degrees.

while one of the TiC stretching vibrations, which is actually coupled with a CCH deformation (see ω_{13} and ω_{14}) gives rise to a medium intense absorption. A relatively intense band is predicted to be at 720 cm^{-1} (ω_5) and corresponds to a mixture of TiH_2 and CCH deformations.

We note that the B3LYP functional calculations yielded with both type of basis sets (see section II) a C_{2v} minimum for the $H_2Ti(C_2H_2)$ molecule, but the low frequency obtained for the TiH_2 wagging mode ($\omega_{15} = 104$ cm^{-1}) indicates again that the wagging potential is rather flat. Apart from this, the computed structural parameters did not vary much with the functional, for instance, the TiC and TiH bond lengths were calculated to be 1.989 and 1.743 Å, respectively. It should be mentioned that Gaussian 94 calculations at the BP86 level resulted in a C_s equilibrium geometry, similar to deMon calculations, showing that the symmetry of the optimized structure does not depend upon the technical aspects of the calculations, but rather on the applied functional.

IV. Identification of the Reaction Products

In what follows now, we will try to identify the structure of the observed species and propose vibrational assignments.

A. Species A: The $H_2Ti(C_2H_2)$ Molecule. The two ^{12}C species bands at 1610.6 and 1585.4 cm^{-1} have very little or no $^{13}C/^{12}C$ isotopic shifts (^{13}C species counterparts appear at 1610.1 and 1585.4 cm^{-1}), but are shifted significantly down to 1158 and 1152.1 cm^{-1}, respectively, with deuterium substitution. Moreover, as mentioned before, the characteristic titanium isotopic structure can be observed for these bands (Figure 4) when they are narrowed by a slight annealing.

With the CH_2CD_2 isotopic precursor, species A displayed two new bands at 1597.3 and 1155.3 cm^{-1}, which represent about the average positions between the peaks at 1610.6 and 1585.4 cm^{-1} with C_2H_4, or at 1158 cm^{-1} and 1152.1 cm^{-1} with C_2D_4. This demonstrates two facts: First, this molecule contains two equivalent, vibrationally coupled Ti−H(D) bonds. Second, it shows that the Ti atom abstracts one hydrogen (or deuterium) from each carbon. Any other possibility would have yielded more signals in each (TiH or TiD) region.

The 1464.8 cm^{-1} band has a large $^{12}C/^{13}C$ shift of 50.8 cm^{-1}, which is only 15% smaller than the value of 59.8 cm^{-1} calculated for the $^{12}C/^{13}C$ isotopic shift of a pure C−C stretching motion at this frequency. The 1464.8 cm^{-1} band should thus be assigned to a vibration involving mostly the C−C coordinate, but mixing with some other vibrational components. Using C_2D_4 precursor, this band shifts by 67.2 cm^{-1}, and with CH_2-CD_2 the shift is reduced to 29 cm^{-1}, that is, about halfway between the C_2H_4 and C_2D_4 values. This shows a notable, but relatively small, contribution of hydrogen (or deuterium) motion in the vibration. Note that the H/D effect on the ν_2 vibration of free ethylene (having the most C═C stretching character) is about 110 cm^{-1}, about twice as large as the shift observed here. This is consistent with a smaller number of hydrogens born on each carbon. The single signal observed with the CH_2CD_2 precursor presents, however, a shift intermediate between the C_2H_4 and C_2D_4 values, showing that the C═C bond still bears one hydrogen and one deuterium in equivalent positions. The perturbation of the C═C motion in comparison with free ethylene is substantial, but notably less than in a classical π-complex without hydrogen-shift (such as NiC_2H_4, PdC_2H_4). All this shows that species A has a structure corresponding to the $H_2Ti(C_2H_2)$ molecule with a tetracoordinated Ti atom having displaced one hydrogen atom from each carbon of C_2H_4 (see Figure 7). On the ground of the observed isotopic shifts and the predicted harmonic frequencies, we can make preliminary attributions for the other observed frequencies as follows.

The peak at 1000.4 cm^{-1}, for which we get a large shift (128.2 cm^{-1}) upon deuterium substitution, is the out-of-plane CCH deformation mode. This band is predicted at 1015 cm^{-1}, with a C_2H_4/C_2D_4 isotopic shift very close to the observed value (128 vs 135 cm^{-1}).

The absorptions at 765.4 and 687.8 cm^{-1}, presenting very small $^{12}C/^{13}C$ shifts (0.3 and 2.9 cm^{-1}) can be assigned to the symmetric TiH_2 bending and CCH bending motions. The calculated frequencies for these two modes are 751 and 720 cm^{-1} and their relative intensities match well the experimental data. The observed C_2D_4 counterparts should then be the peaks at 548.3 and 454.6 cm^{-1}.

The weak band observed at 667.7 cm^{-1} can be identified as the HCCH out-of-plane deformation, since the 598.1 cm^{-1} band, with its relatively large $^{12}C/^{13}C$ effect (12.3 cm^{-1}), is likely to be a TiC stretching mode. The corresponding DFT predictions are 653 and 620 cm^{-1} with reasonable IR intensities and isotopic shifts. For the latter mode, the normal coordinate analysis reveals some contribution from the CCH deformation motion.

The low-frequency bands below 400 cm^{-1} have very small $^{12}C/^{13}C$ shifts and might be assigned to the vibrations of the TiH_2 group as the carbon atom takes little part in these motions. On the basis of the calculated frequencies, we attribute the 399 and 277 cm^{-1} bands to TiH_2 rock and TiH_2 wag, but we recall the uncertainty associated with the calculated values.

Table 5 presents the proposed assignments and a comparison of the theoretical frequencies and isotopic shifts with the experimental data. Experimentally, only relative intensities can be estimated, and with a limited accuracy (about 5% for the strong bands and more than 30% for the weaker and broader signals), and only relative intensities are presented here. The overall agreement between calculated and observed frequencies and isotopic is quite convincing. The mean absolute deviation of the calculated frequencies from experimental values is 26

TABLE 5: Experimental and Calculated Vibrational Frequencies and Isotopic Shifts (both in cm^{-1}) for the $H_2Ti(C_2H_2)$ Molecule[a]

	$H_2Ti(C_2H_2)$		$H_2Ti(^{13}C_2H_2)$		$D_2Ti(C_2D_2)$		HDTi(CHCD)	
	expt	calc	expt	calc	expt	calc	expt	calc
ω_1		3077 (0.00)		12		772		30
ω_2	1611 (0.38)	1647 (0.52)	0.5	0.2	453	476	13	4
ω_3	1465 (0.08)	1448 (0.03)	51	53	67	58	30	31
ω_4	765 (0.06)	751 (0.05)	0.3	0.3	217	215	88	72
ω_5	688 (0.21)	720 (0.27)	2.9	4.5	233	254	48	65
ω_6		571 (0.03)		12		−79[b]		61
ω_7		895 (0.00)		9.5		178		64
ω_8		285 (0.13)		2.1		59		20
ω_9	1585 (1.00)	1639 (1.00)	0.0	0.0	433	459	431	463
ω_{10}	668 (0.07)	653 (0.07)	4.5	4.6	179	148	147	111
ω_{11}	399 (0.17)	429 (0.02)	1.0	0.7	107	116		72
ω_{12}		3041 (0.01)		9.3		804		758
ω_{13}	1000 (0.05)	1015 (0.18)	23	19	128	135		43
ω_{14}	598 (0.16)	620 (0.19)	12	12	91	114	26	44
ω_{15}	277 (0.06)	248 (0.59)	0.2	0.5	75	64	58	52

[a] Relative IR intensities (in parentheses) are given with respect to the most intense absorption. [b] Inverse isotopic shift (frequency shifted to higher frequency).

cm^{-1}, which is remarkably small. The average error of the B3LYP calculations is somewhat larger (58 cm^{-1}), but it should be noted that most of the error comes from the overestimation of the two TiH stretching frequencies (ω_2 and ω_9) and the discrepancy obtained for the TiH_2 wagging mode (ω_{15}).

Particularly meaningful is the correct reproduction of the vibrations involving the C−C bond (around 1465 cm^{-1}, thus confirming a double bond character) and the TiH_2 group (with correct ordering, isotopic shifts and intensity ratios of the very strong TiH stretching modes ν_2 and ν_9). The assignment of the 1611 cm^{-1} band as ν_2 is confirmed by the small $^{12}C/^{13}C$ isotopic shift due to small vibrational coupling with the close-lying ν_3 C═C stretching motion. The positions of the low-frequency modes are quite adequately reproduced as well, even though the relative intensities of the weaker bands are only approximate. Noteworthy are first the relatively high positions of the TiH_2 bending mode (around 765 cm^{-1}, as compared to less than 500 cm^{-1} in the triatomic dihydride molecule or 637 and 547 cm^{-1} for the tetrahydride)[6,7] and, second, the frequencies of the motions involving mostly the Ti−C bonds around 600 cm^{-1}. For this molecule, this translates into a Ti−C bond force constant of the order of 2.9 ± 0.1 mdyn/Å, which is noticeably larger than in $Ti(CH_3)_4$ (2.28 mdyn/Å).[29]

Regarding the structure of the $H_2Ti(C_2H_2)$ molecule, a comparison with the highly strained, but room-temperature-stable cyclopropene molecule can be made. Although the C−C bond is about 0.04 Å shorter in C_3H_4[30] than in $H_2Ti(C_2H_2)$, the C═C double bond character of the C_2H_2 unit in $H_2Ti(C_2H_2)$ is evident from the calculated carbon−carbon bond orders: 1.75 and 1.85 in $H_2Ti(C_2H_2)$ and C_3H_4, respectively. Also, the calculated Ti−C and Ti−H bond orders seem to indicate strong Ti−C and Ti−H bonds. These bonds, however, are not purely covalent as opposed to C−C and C−H in C_3H_4,[31] because the Ti atom in $H_2Ti(C_2H_2)$ possesses a notable amount of positive charge (Q(Ti) = +0.58 e, as obtained from Mulliken population analysis). More than two-third of the corresponding negative charge (−0.34 e) is distributed on the C_2H_2 unit, and the Ti-coordinated H atoms are negatively charged as well. Both the Ti−C and Ti−H bonds thus have some ionic character.

Some organometallic species also provide interesting reference points. If TiH_4[6,7] or $Ti(CH_3)_4$[29] is generally assumed or calculated to be tetrahedral, the structures of more closely related organometallic molecules containing titanacyclopropenylium three-membered rings such as $Cp_2Ti(C_2X_2)$[32−35] (with X = C_6H_5, CH_3) are not precisely known. Only for the diphenyl-cyclopropenyliumtitanocene species a C═C distance around 1.3 Å could be ascertained.[34]

The calculated Ti−C distances are remarkably short (∼1.97 Å) compared to standard Ti−C distances in tetraaryl compounds[36] (2.13 Å). This is corroborated by the results of the normal coordinate analysis based on the experimental data showing here a Ti−C force constant of the order of 2.87 mdyne $Å^{-1}$.

In the various bicyclopentadienyl compounds where the titanium is tetracoordinated, the metal is usually regarded as occupying the vertex of a tetrahedron, although crystallographic data show a significant amount of distortion (the "bond" angle between the centroids of the cyclopentadienyl groups and the metal atom are normally around 130°). The situation here is obviously different, since the ∠CTiC bond angle is very accute (calculated around 40°), and it is the ∠HTiH bond angle which opens up above 120°, a value still significantly lower than the valence bond angle calculated in TiH_2 (140 to 142° in the $^3B_1$ ground state).[32,37]

B. Species B: The $HTi(C_2H_3)$ Molecule. Unlike for species A, only one strong absorption was found in the TiH stretching vibrational region for species B. This absorption lies substantially lower in energy (1500 cm^{-1} with C_2H_4 precursor) than the two TiH stretching modes in $H_2TiC_2H_2$. Earlier studies have shown that the Ti−H stretching frequency in TiH_x molecules increases following the number of titanium valence bonds. For instance, in the TiH, TiH_2, TiH_3, TiH_4 series, the average Ti−H stretching frequencies are 1385, 1460, 1600, and 1660 cm^{-1}, respectively.[6,7] For this reason, species B seems to contain one Ti−H bond, born by a di- or trivalent Ti atom. The band observed around 580 cm^{-1} (14.1 cm^{-1} $^{12}C/^{13}C$ shift) is then a good candidate for the Ti−C stretching vibration. This value is also lower than the Ti−C stretching frequency in the $H_2TiC_2H_2$ molecule, where the Ti atom is tetravalent. Considering the fact that species B can be converted to $H_2TiC_2H_2$ (see section III.A), its stochiometric formula should be $HTiC_2H_3$.

DFT calculations presented in section III.B predict two different structures (i.e., the singlet state titanacyclopropene and the triplet state vinyl titanium monohydride) for $HTiC_2H_3$, having fairly similar stabilities. Assuming that the band observed at 1569 cm^{-1} with the $^{13}C_2H_4$ precursor is due to a CC stretching vibration, one could associate species B with the vinyl hydride structure. The existence of low-frequency bands around 200 cm^{-1} in the IR spectra is also more consistent with the vinyl hydride structure, since no band is expected in this

TABLE 6: Experimental and Calculated Vibrational Frequencies and Isotopic Shifts (both in cm^{-1}) for the $HTi(C_2H_3)$ Molecule[a]

	$HTi(C_2H_3)$		$HTi(^{13}C_2H_3)$		$DTi(C_2D_3)$		$HTi(CHCD_2)$		$DTi(CDCH_2)$	
	expt	calc	expt	calc	expt	calc	expt	calc	expt	calc
a′										
ω_1		3080 (0.00)		11		794		2.4		32
ω_2		3045 (0.01)		9.3		802		791		−0.3
ω_3		2764 (0.11)		6.7		742		742		769
ω_4	1500 (1.00)	1586 (1.00)	0.0	0.6	420	454	−0.3	1.1	418.8	454
ω_5		1560 (0.11)		20		152		138		2.6
ω_6		1358 (0.12)		36		306		325		16
ω_7		1135 (0.06)		17		188		51		68
ω_8	868 (0.25)	818 (0.07)	0.8	1.7	203	226		99		143
ω_9	582 (0.18)	600 (0.06)	14.1	13	50	63		44		50
ω_{10}	310 (0.27)	358 (0.08)	5.9	4.0	21	26		−13		27
ω_{11}	217 (0.26)	276 (0.20)	−0.5	2.9		65		19		58
a″										
ω_{12}		909 (0.02)		5.1		214		57		104
ω_{13}		772 (0.10)		7.0		171		153		50
ω_{14}	384 (0.23)	399 (0.09)	1.5	2.7	127	115		90		37
ω_{15}		69 (0.10)		0.5		16		3.2		14

[a] Relative IR intensities (in parentheses) are given with respect to the most intense absorption. The normal modes are classified into in-plane (a′) and out-of-plane (a″) vibrations.

region for the more compact ring structure. Moreover, the predicted TiH stretching frequency (1613 cm^{-1}) for the singlet $HTiC_2H_3$ molecule seems too high to correspond to the observed 1500 cm^{-1} value, while that of the triplet structure (1586 cm^{-1}) is closer.

From a comparison of experimental and theoretical IR data (Tables 1 and 3), assignments for the remaining observed bands are proposed. The two medium intense absorptions at 867.7 and 383.6 cm^{-1} with very small $^{12}C/^{13}C$ shifts (0.8 and 1.5 cm^{-1}) and considerable H/D shifts (203 and 127 cm^{-1}) can be attributed to the out-of-phase CH/CH_2 rocking and the TiCC torsional vibrations. The bands observed at 309.6 and 217.0 cm^{-1} are most likely related to the HTiC and TiCC bending motions, calculated to be highly coupled.

Table 6 summarizes the comparison of experimental and theoretical data and the proposed assignments. It is apparent that the match is less satisfactory here than for species A (the average discrepancy between the calculated and experimental frequencies is 46 cm^{-1} and the relative intensities are less consistent), but the level of agreement is still reasonable to associate species B with the vinyl hydride structure. There are, however, a few observed features which cannot be explained from our theoretical results. For instance, we were not able to observe any C−H stretching band, although one is predicted to be relatively intense. Similarly, some predicted bands with appreciable intensities (1358, 1135, and 772 cm^{-1}) were not detected.

A possible explanation for these contradictory results is that the $HTi-(C_2H_3)$ interaction is not adequately described at the present level of theory. The small Ti−C−C bond angle, i.e., the existence of the interaction between Ti and the CH_2 group appears to be rather peculiar in light of the MCPF results reported for the second-row transition metal $HM(C_2H_3)$ series,[38] which showed that the M−C−C angle was always around 120°. Although it has been pointed out that this bond angle is somewhat smaller for early transition metal atoms, no direct $M\cdots(CH_2)$ interaction has been observed for these molecules. The reason for the small Ti−C−C bond angle ($\angle TiCC = 87°$) in $HTi(C_2H_3)$ is yet unclear, but it does not seem to come from the approximation made for the functional and the basis set expansion, since our B3LYP/6-311G** calculations gave very similar structrure to that reported in Table 3. Another possible source of the unusual discrepancies between theory and experiment might be that the matrix effect for this species is so important that it prevents the formation of weak Ti···H and Ti···C interactions.

Concluding Remarks

The experimental material relative to the argon matrix codeposition of Ti atoms and ethylene molecule has demonstrated the existence of two oxidative addition products: (i) an insertion of a Ti atom into a C−H bond to form a vinyl titanium hydride, and (ii) following hydrogen displacement, a metallic cyclic dihydride species. The ground state, equilibrium structures and vibrational frequencies of these species have been determined by DFT calculations. The predicted properties for the $H_2Ti-(C_2H_2)$ molecule is validated by the good agreement between the experimental and theoretically predicted IR data. As for $HTi(C_2H_3)$, the agreement is less satisfactory and points to the necessity of further work. Another unsolved problem of the present study is the absence of the $Ti(C_2H_4)$ species in the IR spectra. As noted before, DFT predicts the $^3B_1$ state of $Ti-(C_2H_4)$ to be strongly bound with a stability comparable to those of the other two species but, despite this, the $Ti(C_2H_4)$ molecule has not been observed in our experiments. A possible explanation for this would be the weak IR intensities predicted for its fundamental vibrations (see Table 2), but this does not seem very convincing in light of other examples with comparable values.[39] Only small amount of hydride species were observed after deposition, and the same species grew after excitation at wavelengths corresponding to Ti atomic transitions. This would indicate that the metal atom had not yet reacted, unless TiC_2H_4 (i) had gone undetected in our experiment and (ii) would also have an electronic transition in the vicinity of the Ti atomic transition. This cannot be excluded, especially considering that both hydride products have low-lying excited states, some of which are 2−3 eV above the ground states and are responsible for the mono- to dihydride conversion. Clearly, further experimental and theoretical works is required.

Acknowledgment. I.P. acknowledges the support of the Hungarian Research Fundation (OTKA, Grant T020231).

References and Notes

(1) Gavens, P. D.; Bottril, M.; Kelland, J. W.; McMeeking, J. In *Comprehensive organometallic Chemistry*; Pergammon Press: Oxford, 1982; Vol. 3.

(2) Cloke, F. G. In *Comprehensive Organometallic Chemistry II*; Abel, E. A., Stone, G. G., Wilkinson, G., Eds.; Elsevier: London 1995; Vol. 4, p 213.
(3) Anthony, M. T.; Green, M. L. H.; Young, D. *J. Chem. Soc., Dalton Trans*. **1975**, 1419.
(4) Hawker, P. N.; Kündig, E. P.; Timms, P. L. *J. Chem. Soc., Chem. Commun*. **1978**, 730.
(5) Morand, P. D.; Francis, C. G. *Inorg. Chem*. **1985**, *24*, 56.
(6) Xiao, Z. L.; Hauge, R. H.; Margrave, J. L. *J. Phys. Chem*. **1991**, *95*, 2696.
(7) Chertihin, G. V.; Andrews, L. *J. Am. Chem. Soc*. **1994**, *116*, 8322.
(8) Mascetti, J.; Tranquille, M. *J. Phys. Chem*. **1988**, *92*, 2177.
(9) Chertihin, G. V.; Andrews, L. *J. Am. Chem. Soc*. **1995**, *117*, 1595.
(10) Atkinson, J. G.; Fisher, M. H.; Horley, D.; Morse, A. T.; Stuart, R. S.; Symes, E. *Can. J. Chem*. **1965**, *43*, 1614.
(11) Becke, A. D. *Phys. Rev. A* **1988**, *38*, 3098.
(12) Perdew, J. P. *Phys. Rev. B* **1986**, *33*, 8822; erratum in *Phys. Rev. B* **1986**, *38*, 7406.
(13) Godbout, N.; Andzelm, J.; Salahub, D. R.; Wimmer, E. *Can. J. Chem*. **1992**, *70*, 560.
(14) Sim, F.; Salahub, D. R.; Chin, S.; Dupuis, M. *J. Chem. Phys*. **1991**, *95*, 4317.
(15) Salahub, D. R.; Fournier, R.; Mlynarski, P.; Pápai, I.; St-Amant, A.; Ushio, J. In *Density Functional Methods in Chemistry*, Labanowski, J., Andzelm, J., Eds.; Springer-Verlag: New York, 1991.
(16) St-Amant, A. Ph.D. Thesis, Université de Montréal, 1991.
(17) St-Amant, A.; Salahub, D. R. *Chem. Phys. Lett*. **1990**, *169*, 387.
(18) Becke, A. D. *J. Chem. Phys*. **1993**, *98*, 5648.
(19) Lee, C.; Yang, W.; Parr, R. G. *Phys. Rev. B* **1988**, *37*, 785.
(20) Frisch, M. J.; Trucks, G. W.; Schlegel, H. B.; Gill, P. M. W.; Johnson, B. G.; Robb, M. A.; Cheeseman, J. R.; Keith, T.; Petersson, G. A.; Montgomery, J. A.; Raghavachari, K.; Al-Laham, M. A.; Zakrzewski, V. G.; Ortiz, J. V.; Foresman, J. B.; Peng, C. Y.; Ayala, P. Y.; Chen, W.; Wong, M. W.; Andres, J. L.; Replogle, E. S.; Gomperts, R.; Martin, R. L.; Fox, D. J.; Binkley, J. S.; Defrees, D. J.; Baker, J.; Stewart, J. P.; Head-Gordon, M.; Gonzalez, C.; Pople, J. A. *Gaussian 94*; Gaussian, Inc.: Pittsburgh, PA, 1995.
(21) Barone, V. *Chem. Phys. Lett*. **1995**, *233* 129.
(22) Barone, V. *J. Phys. Chem*. **1995**, *99* 11659.
(23) Barone, V.; Adamo, C.; Mele, F. *Chem. Phys. Lett*. *1996*, *249* 290.
(24) Fournier, R.; Pápai, I. In *Recent Advances in Density Functional Methods*; Chong, D., Ed.; World Scientific: Singapore, 1995; Part I.
(25) Pápai, I. *J. Chem. Phys*. **1995**, *103*, 1860.
(26) Gruen, D. M.; Carstens, D. H. W. *J. Chem. Phys*. **1971**, *54*, 5206.
(27) The present approach erroneously predicts the $s^1d^3(^3F)$ state of Ti to lie about 7 kcal/mol below the true ground state ($s^2d^2(^3F)$). This error is likely present in the calculated binding energy as well, since the bond formation between the ground-state Ti and C_2H_4 involves s−d hybridization leading to an approximately s^1d^3 atomic configuration in the $^3B_1$ state of $Ti(C_2H_4)$.
(28) Blomberg, M. R. A.; Siegbahn, P. E. M.; Svensson, M. *J. Phys. Chem*. **1992**, *96*, 6, 9794.
(29) Eysel, H. H.; Siebert, H.; Groh, G.; Berthold, H. J. *Spectrochim. Acta* **1970**, *26A*, 1595.
(30) The present method gives $R_{(C=C)} = 1.302$ Å and $R_{C-C} = 1.505$ Å for the cyclopropene molecule, which are close to the experimental values, see: Kasaï, P. H., Myers, R. J., Egers, D. F., Wiberg, K. B. *J. Chem. Phys*. **1958**, *30*, 512.
(31) Hagen, G. *Acta Chem. Scand*. **1969**, *23*, 2311.
(32) Ma, B.; Collins, C. L.; Schaeffer, H. F. *J. Am. Chem. Soc*. **1996**, *118*, 870.
(33) Shur, V. B.; Burlakov, V. V.; Vol'pin, M. E. *J. Organomet. Chem*. **1988**, *347*, 77.
(34) Woo, L. K.; Hays, J. A.; Jacobson, R. A.; Day, C. L. *Organometallics* **1992**, *10*, 2102.
(35) Alt, H. G.; Herrman, G. S. *J. Organomet. Chem*. **1990**, *390*, 159.
(36) Bassi, I.; Allegra, G.; Scordamaglia, R.; Chiccola, G. *J. Am. Chem. Soc*. **1971**, *93*, 3787.
(37) Kudo, T.; Gordon, M. S. *J. Chem. Phys*. **1995**, *102*, 6806.
(38) Siegbahn, P. E. M.; Blomberg, M. R. A.; Svensson, M. *J. Am. Chem. Soc*. **1993**, *115* 1952.
(39) Lee, Y. K.; Hannachi, Y.; Xu, C.; Andrews, L.; Manceron, L. *J. Phys. Chem*. **1996**, *100*, 11228.